

FEB 1 1980

Item 830-H-13

NASA 1609

COMPLETED

NASA Technical Paper 1609

ORIGINAL

Scanning-Electron-Microscope  
Study of Normal-Impingement  
Erosion of Ductile Metals

William A. Brainard and Joshua Salik

JANUARY 1980

ORIGINAL

NASA

(11)

**NASA Technical Paper 1609**

**Scanning-Electron-Microscope  
Study of Normal-Impingement  
Erosion of Ductile Metals**

**William A. Brainard and Joshua Salik**  
*Lewis Research Center*  
*Cleveland, Ohio*



National Aeronautics  
and Space Administration

**Scientific and Technical  
Information Office**

1980

## Summary

Scanning electron microscopy was used to characterize the erosion of annealed copper and aluminum surfaces produced by both single- and multiple-particle impacts. Macroscopic 3.2-millimeter-diameter steel balls and microscopic, brittle erodant particles were projected by a gas gun system so as to impact at normal incidence at speeds up to 140 meters per second. During the impacts by the larger steel balls, extensive deformation leading to extrusion, fracture of surface layers, and adhesive material transfer to the steel ball were observed. During the impacts by the brittle erodant particles, at lower speeds, the erosion behavior was similar to that observed for the larger steel balls. At higher velocities, particle fragmentation and the subsequent cutting by the radial wash of debris created a marked change in the erosion mechanism.

## Introduction

The erosion behavior of ductile metals has been studied by many investigators, notably Finnie (refs. 1 to 3), Tilly (refs. 4 to 8), and Bitter (refs. 9 and 10). These and other researchers have attempted to treat erosion analytically by fitting data to mathematical expressions containing empirical parameters and relating these expressions to a concept of a mechanism. For example, Finnie believes that cutting by the erodant particles should form the basis for an analytical treatment; Tilly suggests that erodant fragmentation must be considered; and Bitter suggests deformation behavior must be considered, particularly for normal incidence. Surprisingly little work on the erosion of ductile metals studied by scanning electron microscopy has been reported.

This investigation was conducted to study the erosion process of ductile metals at a normal angle of incidence by scanning electron microscopy. Both single- and multiple-particle impingement experiments were performed. The eroded surfaces and the erodant particles were examined, and evidence for erosion mechanisms was obtained.

## Apparatus and Procedure

Two impingement methods were used for these studies. In the first method, a small-muzzle gas gun

of a design suggested by Hutchings (ref. 11) was used to accelerate a plastic sabot. A schematic is shown in figure 1. Inside the end of the sabot was either a single 3.2-millimeter-diameter, hardened (700 to 900 kg/mm<sup>2</sup>) AISI 52100 steel ball or a small charge (~4 mm<sup>3</sup>) of erodant particles: 15-micrometer glass beads, 50-micrometer silicon carbide, or 50-micrometer aluminum oxide. A sample of the ductile metal to be eroded was mounted in a holder with the surface normal to the muzzle direction. The velocity of the steel ball was directly measured by a photo-optical gate assembly, and the erodant compact particles were assumed to have approximately the same velocity as that measured for the steel ball when the gas gun was operated under the same pressure.

In the second method, an industrial air abrasive machine, with the same erodant particles as in the first method, was used. In this machine a carrier gas at high pressure (in this case, argon at 80 psi) flows through a nozzle (1.18 mm diam) and accelerates the particles toward the surface of the ductile metal sample mounted normal to the particle stream. No measurement of actual particle velocities was made with this particular machine.

The ductile metals used for these experiments were annealed, oxygen-free, high-conductivity (OFHC) copper and annealed 6061 aluminum alloy (Al-1.0Mg-0.6Si-0.25Cu-0.25Cr). The hardness values were 57 kg/mm<sup>2</sup> for the annealed copper and 37.5 kg/mm<sup>2</sup> for the annealed aluminum alloy.

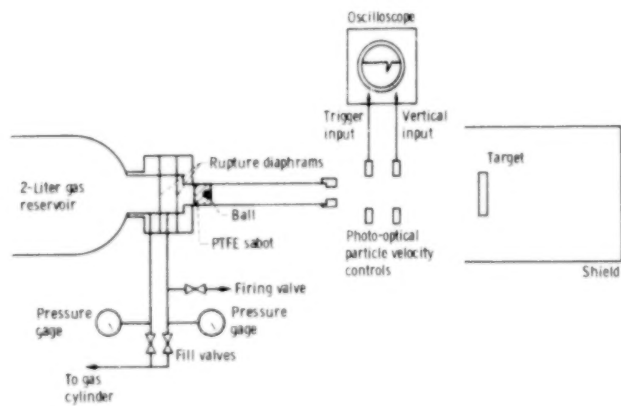


Figure 1. - Schematic of single-particle impingement apparatus.



(a) Top view.



(b) Central cross section

Figure 2 - Annealed copper surface after multiple impacts by 3.2-millimeter-diameter steel ball at 140 meters per second.

## Results

### Steel-Ball Impacts

Both single and multiple impacts into the surface of the annealed copper and aluminum alloy samples were performed. It was of interest to determine from SEM (scanning electron microscopy) observation whether or not the mechanisms for the smaller erodant particles were similar to those observed for the larger steel balls.

Following impact, the sample surfaces and the steel balls were examined in the SEM to observe impact damage. Figure 2 shows two views of a multiple-impact region on a copper surface: a top view and a section through the center of the impact region. The impacts were at a speed of 140 meters

per second. Of particular interest are the region between two adjacent impacts and the region below (subsurface) the impact zone. Figure 3 presents higher magnification micrographs, in this case from an aluminum surface, of the extruded metal peaks. Note in particular the extensive cracking and the layer-like structure. Very thin lamellae of aluminum were observed to occur on the sides and bottoms of impact craters (fig. 4). Such lamellae are likely to be easily detached on subsequent impacts. Transfer of aluminum in very thin layers to a steel ball on impact had been confirmed by X-ray analysis (ref. 12). The amount of transferred material per impact seemed to increase with the number of impacts.

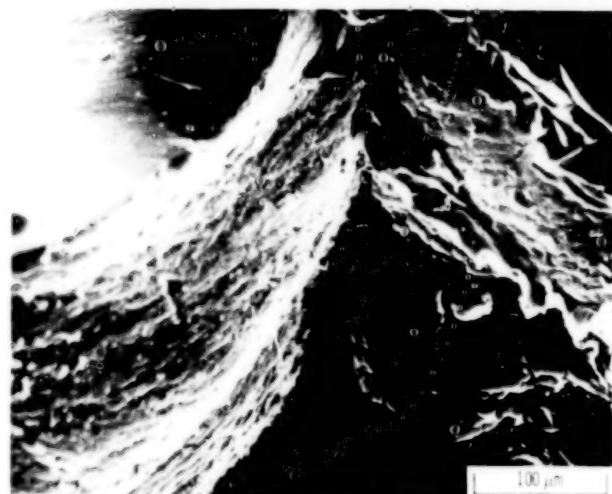


Figure 3 - Annealed 6061 aluminum surface after adjacent impacts by 3.2-millimeter-diameter steel ball at 140 meters per second.

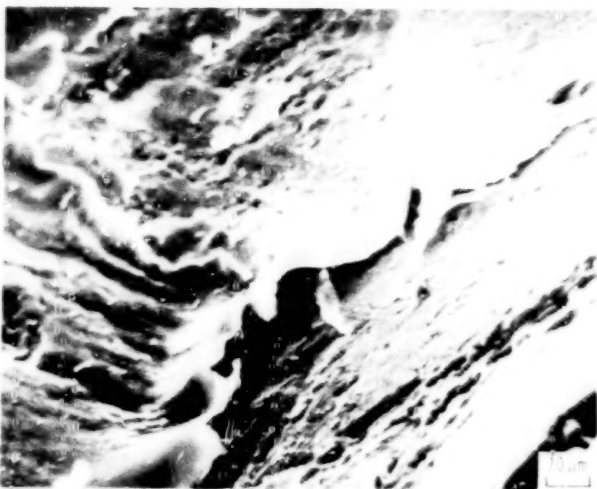


Figure 4. - Annealed 6061 aluminum surface after six impacts by 3.2-millimeter-diameter steel ball at 140 meters per second

The lamellae were not observed for copper. Rather, copper exhibits the formation of a thicker, highly deformed layer (fig. 5) and, with repeated impacts, both lateral and transverse cracking (fig. 6). Adhesive transfer of copper to the steel ball occurs, and the amount appears to increase with the number of impacts (i.e., the amount per impact increases with total number of impacts). There is clear evidence of tensile fracture in the copper as a result of adhesion during impact. The micrograph of figure 7 shows a region near the bottom of an impact crater made in an annealed copper sample that had been impacted several times. A layer of material nearly 1 micrometer thick had been removed. Analogous pictures of the ball surface after this impact are shown in figure 8. The X-ray map

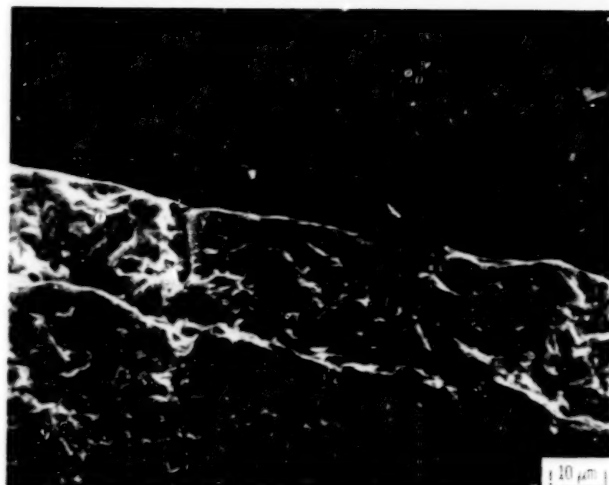


Figure 5. - Central cross section of bottom of impact crater in annealed copper made by 3.2-millimeter-diameter steel ball at 93 meters per second. Etched in nital.

clearly shows a rather heavy film of copper transferred onto the steel surface. It is likely that, with repeated impacts, fracture is more extensive because of the presence of cracks from previous impacts. No marked change in mechanisms could be inferred for either copper or aluminum as the number of impacts increased.

#### Erodant-Particle Impacts

Most erosion-causing particles in actual operating systems are considerably smaller and more angular than the steel balls used for the experiments described in the previous section. To observe if there were differences between the larger steel balls and actual erodant particles, the surfaces of annealed copper and aluminum samples were impacted by compacts of erodant particles of aluminum oxide and silicon carbide and glass beads. Figure 9 shows micrographs of silicon carbide particles and glass beads. The aluminum oxide particles were similar to the silicon carbide particles in size and shape.

Tilly, et al. (refs. 7 and 8) have discussed erosion as a two-stage process consisting of the primary impact and secondary fragmentation effects. These researchers showed that the extent of fragmentation depends on particle size, shape, and velocity. In the experiments reported herein, significant particle fragmentation was observed to occur (fig. 10). Clearly, cutting and plowing by the debris is a significant mechanism in such situations. A velocity of 140 meters per second corresponds to the lower end of the data published by Tilly regarding percent fragmentation versus velocity. However, those

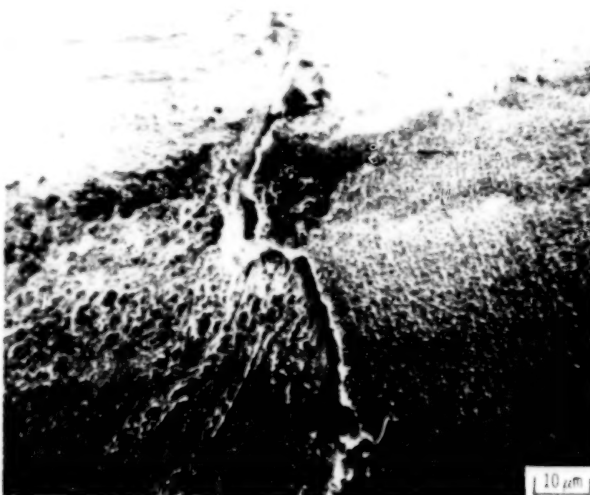
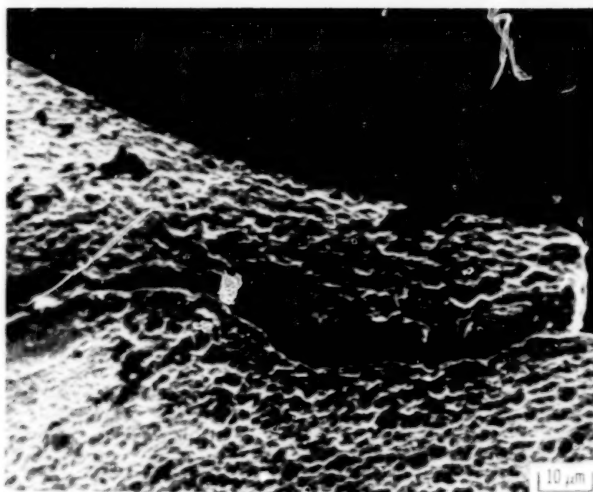


Figure 6. - Central cross section of multiple-impact region in annealed copper after impacts by 3.2-millimeter-diameter steel ball at 140 meters per second.

data were for 125- to 150-micrometer quartz particles. In addition to fragmenting, the smaller erodant particles, particularly the angular particles, often become embedded in the ductile metal surfaces (fig. 11). This effect has been reported before and accounts for initial weight gains reported in some experimental studies of erosion (ref. 13).

Surfaces of aluminum that were eroded both by gas gun at 93 meters per second and by exposure to the stream produced by an industrial air abrasive machine are shown in figure 12. Both surfaces were eroded by the same-size spherical glass beads. Clearly, the surface resulting from bombardment by means of the gas gun is more severely damaged, and both particle fragmentation and embedment have occurred. The surface resulting from bom-

bardment by means of the industrial machine exhibits overlapping, plastically deformed craters without any evidence of particle fragmentation. This suggests that although the gas-stream velocity through the nozzle may be rather high, the actual particle velocity may be much lower. This was confirmed by Neilson and Gilchrist (ref. 14), who actually measured the erodant particle velocities photoelectrically and compared those values with the calculated efflux velocity of the gas stream. They found that the particle velocity, depending on the particle mass to gas mass ratio, could be less than one-fourth the efflux velocity.

When glass beads were replaced with silicon carbide particles in the industrial air abrasive machine, significant particle fragmentation occurred under the same conditions. The extent of fragmentation

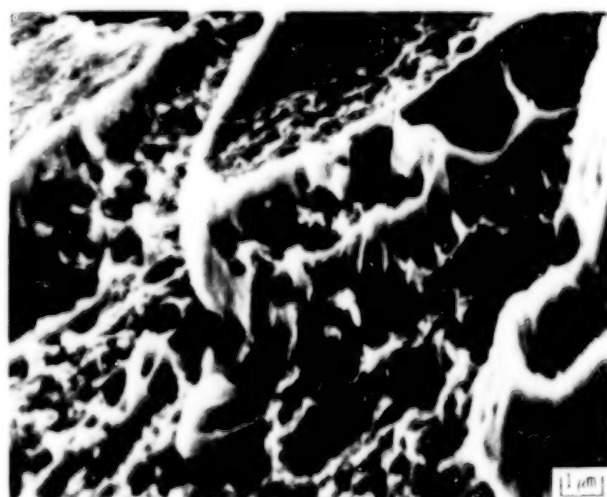
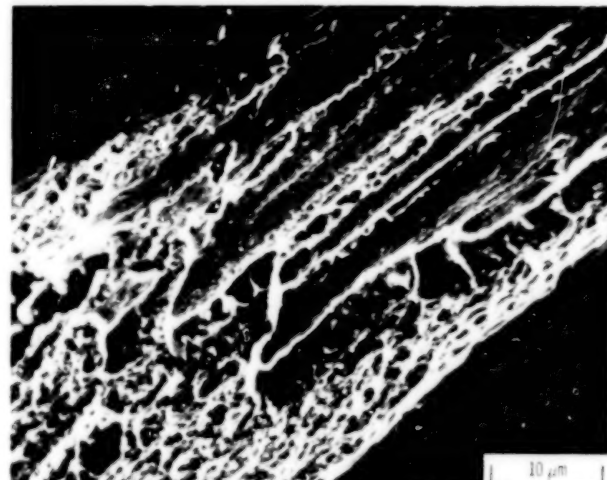
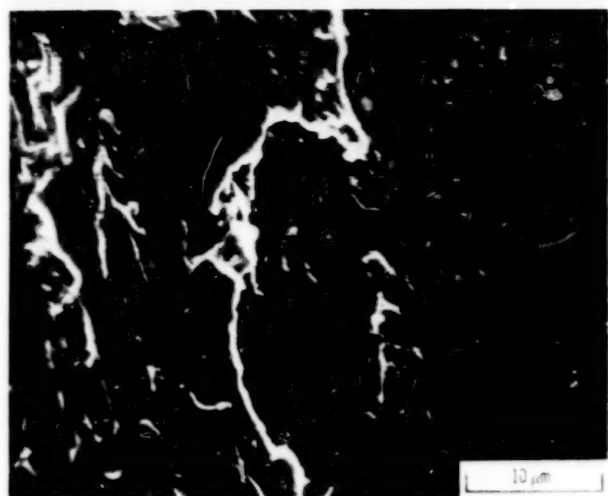


Figure 7. - Bottom of crater in annealed copper surface after five impacts by 3.2-millimeter-diameter steel ball at 140 meters per second.



(a) Scanning electron micrograph.



(b) Copper  $K_{\alpha}$  map.

Figure 8. - 3.2-Millimeter-diameter steel ball after 140-meter-per-second impact into annealed copper previously impacted four times.

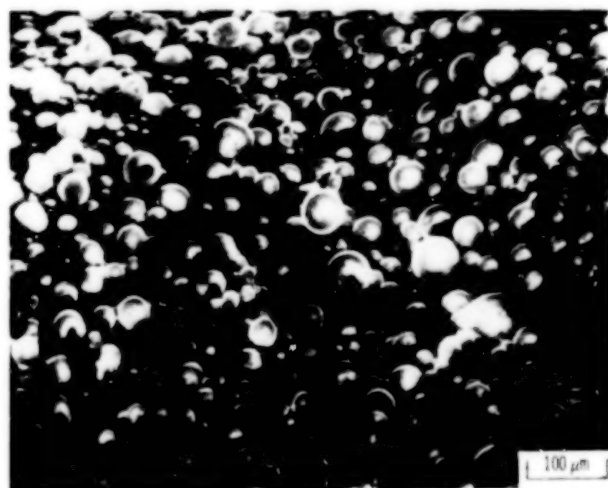
was such that light was emitted from a metal surface being struck by the stream of silicon carbide particles. Light is emitted as a result of fracture of silicon carbide (ref. 15). Silicon carbide probably fragments because of the uneven stress distribution on the sharp, angular silicon carbide particles. This is in contrast to the glass beads, which are round. The fragmentation is responsible in part for the higher erosion rate produced with silicon carbide as compared with glass beads.

The surface of aluminum after long exposure to the machine-produced, glass-bead stream is shown in figure 13. Ripples are observed on the eroded surface as reported and discussed by Finnie and Kabil (ref. 1). Higher magnification reveals the

lamellar structure that was observed for the impact of steel balls onto aluminum. This suggests that the prominent mechanism under those conditions is a deformation-induced fracture of surface layers. Since significant adhesion and material transfer occur for the steel-ball impacts into aluminum and copper, it is likely that adhesion between these smaller erodant particles and the metal may also occur. No evidence for aluminum transfer onto the glass beads was obtained by X-ray, however. For copper eroded by aluminum oxide particles, significant amounts of copper were detected on the "used" particles (fig. 14). For aluminum eroded by glass beads, it is likely that any transfer, if occurring, is in layers too thin to be detected by electron-beam-induced X-ray analysis but able to

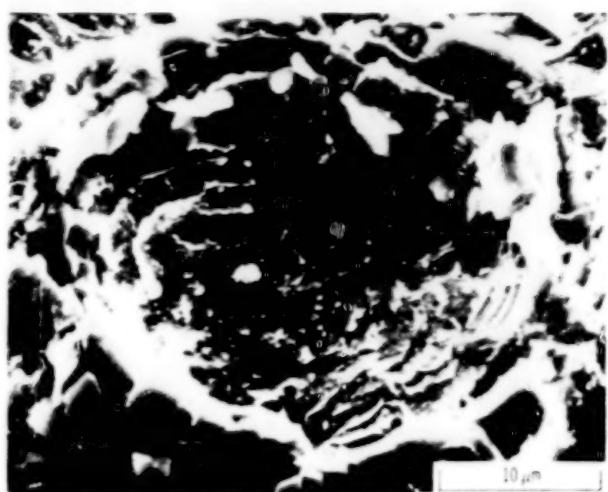


(a) Silicon carbide particles.

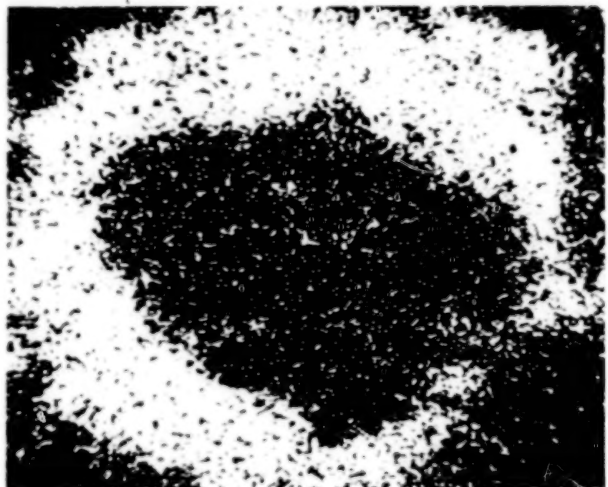


(b) Glass beads.

Figure 9. - Erodant particles.



(a) Scanning electron micrograph.



(b) Silicon  $K_{\alpha}$  map.

Figure 10 - Annealed 6061 aluminum surface after impact by glass beads at 140 meters per second.

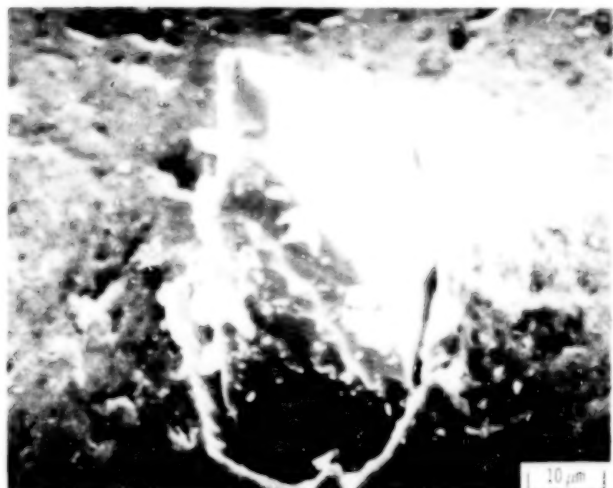
be detected by a more surface-sensitive technique such as Auger spectroscopy or X-ray photoelectron spectroscopy (ref. 16).

### Discussion

The erosion of ductile metals at normal incidence does not have a single responsible mechanism. Rather, many different processes that can occur simultaneously result in material removal. The magnitude of the erosion produced by any one mechanism may vary from inconsequentially small to extremely significant depending on the erosion conditions—such as the angle of impingement and the velocity, type, and size of the erodant particles. Clearly, any theory of erosion that attempts to

predict material loss rates by consideration of only one mechanism will be limited in usefulness.

Fundamental studies on erosion mechanisms have been performed by other investigators on the basis of single-particle impacts of spherical or angular projectiles (refs. 17 to 19). Most of these investigations were conducted at oblique rather than normal incidence, with the result that a cutting mechanism was seen to predominate. At normal incidence the primary impact seems to do very little cutting, and other mechanisms of material removal are involved. At low particle velocity the dominant mechanism seems to be deformation-induced fracture of surface layers. At higher velocities, fragmentation of the particles, depending mainly on the erodant particle shape, occurs and



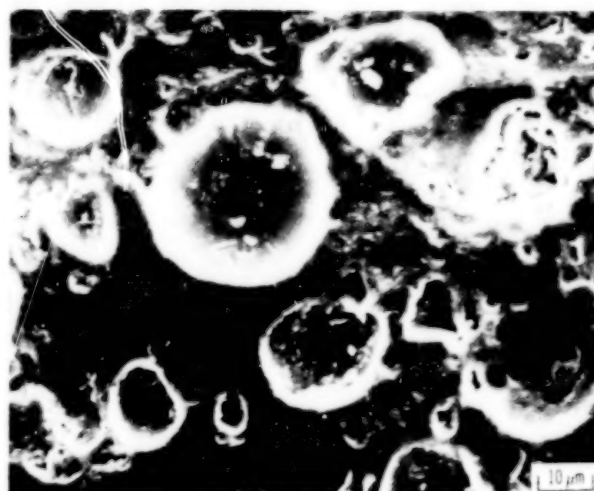
(a) Silicon carbide particle.



(b) Glass bead.

Figure 11 - Erodant particles embedded in 6061 aluminum after impacting at 93 meters per second.

the resulting radial wash of sharp debris results in cutting. Also, as the particle velocity increases, another erosion mechanism, namely adhesive material transfer from the target onto the erodant particles, becomes increasingly significant. As observed earlier (ref. 12) the amount of adhesively transferred material increases with impact velocity, and thus this mechanism of material removal is more significant at high particle velocity. The amount of material removal by adhesive transfer also depends on the combination of erodant and target materials and the degree of target deformation.



(a) Gas gun (impact velocity, 93 m/sec).

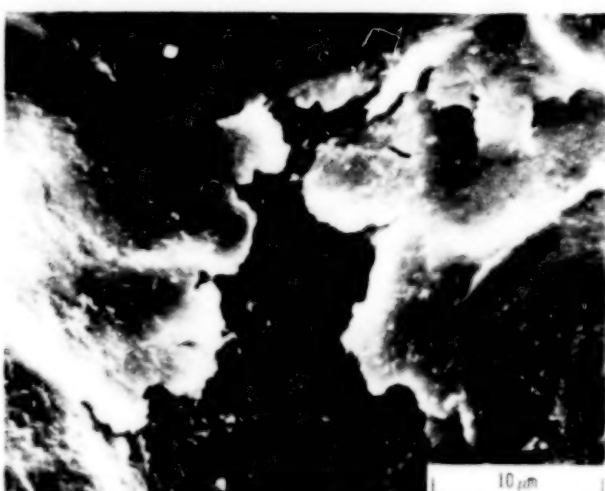
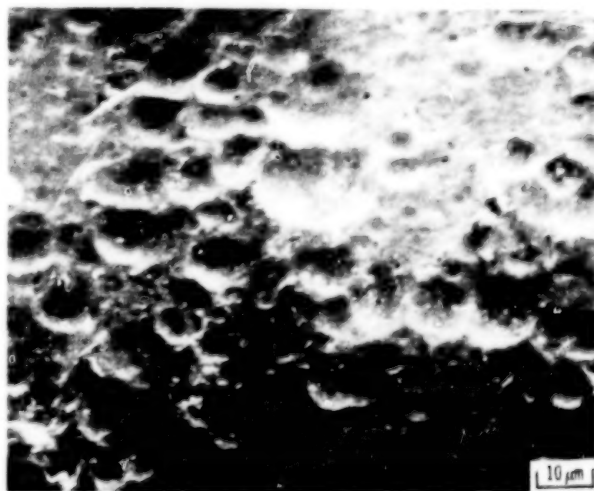


Figure 13 - Erosion crater in 6061 aluminum, produced by glass-bead impact.



(b) Industrial abrasive machine.

Figure 12. - Annealed 6061 aluminum surface eroded by glass beads impinged by two methods.

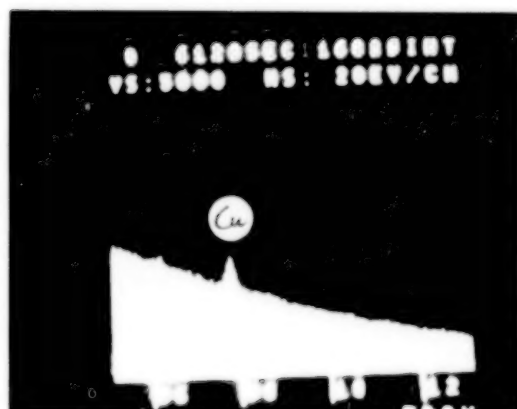


Figure 14. - Energy-dispersive X-ray spectrum of aluminum oxide erodant particles after impact against annealed copper.

## Summary of Results

Extensive examination by scanning electron microscopy of copper and aluminum that had been subjected to erosive impacts revealed many important features. During impact by relatively large steel balls, extensive deformation, extrusion, and adhesive material transfer occurred. The deformed aluminum formed lamellae that could be easily removed on subsequent impacts. Copper experienced tensile fracture because of the strong adhesion bonding.

For high-velocity impacts (~140 m/sec) with brittle, erodant microscopically sized particles (such as glass beads or silicon carbide), particle fragmentation and embedment along with adhesive material transfer from the target onto the erodant particle are the significant features of the erosion process. Cutting of the extruded metal by the fragmentation debris becomes a significant erosion mechanism under such conditions. At lower speeds (~90 m/sec) the main erosion mechanism seems to be fracture of surface layers.

Lewis Research Center,  
National Aeronautics and Space Administration,  
Cleveland, Ohio, September 14, 1979,  
506-16.

## References

1. Finnie, Iain: Erosion of Surfaces by Solid Particles. *Wear*, vol. 3, 1960, pp. 87-103.
2. Finnie, I.; and Kabil, Y. H.: On the Formation of Surface Ripples During Erosion Wear, *Wear*, vol. 8, 1965, pp. 60-69.
3. Finnie, I.; and McFadden, D. H.: On the Velocity Dependence of the Erosion of Ductile Metals by Solid Particles at Low Angles of Incidence. *Wear*, vol. 48, 1978, pp. 181-190.
4. Sage, W.; and Tilly, G. P.: The Significance of Particle Size in Sand Erosion of Small Gas Turbines. *Aeronaut. J.*, vol. 73, May 1969, pp. 427-428.
5. Tilly, G. P.: Erosion Caused by Airborne Particles. *Wear*, vol. 14, 1969, pp. 63-79.
6. Tilly, G. P.: Sand Erosion of Metals and Plastics: A Brief Review. *Wear*, vol. 14, 1969, pp. 241-248.
7. Tilly, G. P.: A Two-Stage Mechanism of Ductile Erosion. *Wear*, vol. 23, 1973, pp. 87-96.
8. Goodwin, J. E.; Sage, W.; and Tilly, G. P.: Study of Erosion by Solid Particles. *Proc. Inst. Mech. Eng.*, vol. 184, pt. 1, no. 15, 1969-1970, pp. 279-292.
9. Bitter, J. G. A.: A Study of Erosion Phenomena—Part I. *Wear*, vol. 6, 1963, pp. 5-21.
10. Bitter, J. G. A.: A Study of Erosion Phenomena—Part II. *Wear*, vol. 6, 1963, pp. 169-190.
11. Hutchings, I. M.; and Winter, R. E.: A Simple-Small-Bore Laboratory Gas-Gun. *J. Phys. E., Sci. Instrum.*, vol. 8, 1975, pp. 84-86.
12. Salik, J.; and Brainard, W. A.: Adhesive Material Transfer in the Erosion of an Aluminum Alloy. *NASA TM-79165*, 1979.
13. Neilson, J. H.; and Gilchrist, A.: Erosion by a Stream of Solid Particles. *Wear*, vol. 11, 1968, pp. 111-122.
14. Neilson, J. H.; and Gilchrist, A.: An Experimental Investigation into Aspects of Erosion in Rocket Motor Tail Nozzle. *Wear*, vol. 11, 1968, pp. 123-143.
15. Wawner, F. E., Jr.; DeBolt, H. E.; and Krukonis, V. J.: Light Emission During the Fracture of Silicon Carbide Filaments. *Silicon Carbide*, 1973, R. C. Marshall, J. W. Faust, Jr., and C. E. Ryan, eds., University of South Carolina Press, 1974, pp. 464-467.
16. Wheeler, D. R.: Principles of ESCA and Application to Metal Corrosion, Coating and Lubrication. *NASA TM-78839*, 1978.
17. Winter, R. E.; and Hutchings, I. M.: Solid Particle Erosion Studies Using Single Angular Particles. *Wear*, vol. 29, 1974, pp. 181-194.
18. Hutchings, I. M.; and Winter, R. E.: Particle Erosion of Ductile Metals: A Mechanism of Material Removal. *Wear*, vol. 27, 1974, pp. 121-128.
19. Sheldon, G. L.; and Kanhere, A.: An Investigation of Impingement Erosion Using Single Particles. *Wear*, vol. 21, 1972, pp. 195-209.

1. Report No. <b>NASA TP-1609</b>	2. Government Accession No.	3. Recipient's Catalog No.	
4. Title and Subtitle <b>SCANNING-ELECTRON-MICROSCOPE STUDY OF NORMAL-IMPINGEMENT EROSION OF DUCTILE METALS</b>		5. Report Date January 1980	
7. Author(s) <b>William A. Brainard and Joshua Salik</b>		6. Performing Organization Code	
9. Performing Organization Name and Address <b>National Aeronautics and Space Administration Lewis Research Center Cleveland, Ohio 44135</b>		8. Performing Organization Report No <b>E-085</b>	
12. Sponsoring Agency Name and Address <b>National Aeronautics and Space Administration Washington, D.C. 20546</b>		10. Work Unit No. <b>506-16</b>	
15. Supplementary Notes <b>William A. Brainard, Lewis Research Center; Joshua Salik, National Research Council - NASA Research Associate.</b>		11. Contract or Grant No.	
16. Abstract  Scanning electron microscopy was used to characterize the erosion of annealed copper and aluminum surfaces produced by both single- and multiple-particle impacts. Macroscopic 3.2-mm-diameter steel balls and microscopic, brittle erodant particles were projected by a gas gun system so as to impact at normal incidence at speeds up to 140 m/sec. During the impacts by the brittle erodant particles, at lower speeds the erosion behavior was similar to that observed for the larger steel balls. At higher velocities, particle fragmentation and the subsequent cutting by the radial wash of debris created a marked change in the erosion mechanism.			
17. Key Words (Suggested by Author(s)) <b>Erosion; Impingement; Ductile metals; Scanning electron microscope</b>		18. Distribution Statement <b>Unclassified - unlimited STAR Category 26</b>	
19. Security Classif. (of this report) <b>Unclassified</b>	20. Security Classif. (of this page) <b>Unclassified</b>	21. No. of Pages <b>10</b>	22. Price* <b>A02</b>

\* For sale by the National Technical Information Service, Springfield, Virginia 22161

NASA-Langley, 1980

